Determination of Surface Tension and Contact Angle from the Shapes of Axisymmetric Fluid Interfaces

Y. ROTENBERG, L. BORUVKA, AND A. W. NEUMANN

Department of Mechanical Engineering, University of Toronto, Toronto, Canada

Received March 5, 1982; accepted August 23, 1982

A general, yet user-oriented scheme is provided to determine liquid–fluid interfacial tensions and contact angles from the shapes of axisymmetric menisci, i.e., from sessile as well as pendant drops. The strategy employed is to construct an objective function which expresses the error between the physically observed and a theoretical Laplacian curve, i.e., a curve representing a solution of the Laplace equation of capillarity. This objective function is minimized numerically using the method of incremental loading in conjunction with the Newton–Raphson method. This strategy is necessary as the otherwise powerful Newton–Raphson method depends on a good initial approximation to the true curve. Incremental loading provides a scheme of approaching the solution from a remote situation. A spherical meniscus, i.e., the case of infinite interfacial tension, is chosen here as the simple, unloaded solution. The method is set up from the point of view of user convenience: Apart from local gravity and densities of liquid and fluid phases the only input information required to determine the liquid–fluid interfacial tension is information on meniscus shape, typically several coordinate points in a coordinate system the origin of which may be placed at will. Specifically it is not necessary to identify the apex of the drop profile, the drop width, or drop height. For determinations of contact angles, the vertical coordinate of the three-phase line needs to be specified. As an illustration, "synthetic" drops, simulating physical drop profiles, are investigated. Sessile drops are generated with the aid of the tables of Bashforth and Adams and pendant drops with the aid of the tables of Fordham. The results show that the technique, which is an absolute one independent of any tables, is fully functional. A computer program implementing the method may be purchased from the authors.

I. INTRODUCTION

The measurement of interfacial tension of fluid interfaces and the measurement of the contact angle which is formed between the fluid interface and a restricting wall are of prime importance in surface science. Several techniques were developed for this purpose and detailed descriptions of the methods can be found in review papers by Padday (1), Ambwani and Fort (2), and Neumann and Good (3). Of all the methods which were developed, the sessile drop method and the pendant drop method emerged as the most general experimental techniques. They are suitable for numerous situations such as experimentation with biological systems, application to systems which show aging effects of interfacial tension, determination of interfacial tension between two liquids, and more.

Despite the experimental simplicity in using sessile and pendant drops for determining interfacial tension and contact angle, there are doubts remaining whenever high accuracy and consistency are needed. Until recently most of the available computational procedures, in conjunction with the above two methods, were limited in the extent to which they could be applied. The two cases of sessile drop and pendant drop were treated separately, and the experimental information had to be interpreted with different sets of tables. Such tables are those of Bashforth and Adams (4) for sessile drops, and of Fordham (5) for pendant drops, as well as other tables (1). The use of the tables is limited to drops of a certain size range and drops of a certain

0021-9797/83 $3.00

shape range (1, 6); in another case (4) the existing tables are unsuitable for drops (sessile drops) of which the contact angle is less than ninety degrees.

Hartland and Hartley collected numerous solutions for determining the interfacial tensions of axisymmetric liquid–fluid interfaces of different shapes and presented the results in tabulated form (7). In their book they reproduced, in a modified form, the existing tables for determining interfacial tensions and contact angles from the shape of sessile and pendant drops and extended these tables to cover a wide range of configurations.

A serious and perhaps the major source of error in these methods is connected with data acquisition. The description of the whole surface of the drop is reduced into the measurements of a few preselected critical points which are compatible with the use of the tables. These points are critical since they correspond to special features, such as inflection points on the interface, and they must be determined with high precision. In addition, if the value of the contact angle is also desired, the location of the contact point, where the three phases meet, must be accurately determined. Such measurements are not at all easily obtained.

In a recent publication, Malcolm and Paynter (8) proposed yet another analytic method for the determination of contact angle and surface tension from sessile drop measurements. However, as with some of the previous approaches the data points are specific geometric points on the drop interface and the method is limited to sessile drops where the contact angle is greater than 90°.

Maze and Burnet (9) started the development of a more satisfactory scheme for the determination of interfacial tension from the shape of sessile drops. They developed a numerical algorithm consisting of a nonlinear regression procedure in which a calculated drop shape is made to fit a number of arbitrarily selected and measured coordinate points on the drop profile, by varying two parameters until a best fit is obtained. In other words, the measured drop shape (one-half of the meridian section) is described by a set of coordinate points and no particular significance has to be assigned to any one of the points. In order to start the calculation, reasonable estimates of the drop shape and size parameters (9) are required; otherwise, the calculated curve will not converge to the measured one. The initial estimates are obtained, indirectly, using the tables of Bashforth and Adams (4).

Despite the progress in strategy, there are several deficiencies in this algorithm:

The error function is computed by summing the squares of the horizontal distances between the measured points and the calculated curve. This measure may not be adequate, in particular, for sessile drop shapes which are strongly influenced by the gravity forces (large drop size at low surface tension). Such shapes tend to flatten near the apex of the drop. Therefore, any data point which is near the apex, may cause a large error even if it lies very close to the "best" curve leading to considerable bias of the solution.

Of equal importance is the location of the apex of the drop, which determines the origin of the calculated curve. Although Maze and Burnet (10) admitted that locating the origin is an important task and have indeed attempted some modifications to their original program, they did so only with respect to adjusting the vertical displacement of the origin but not the horizontal displacement.

In the following section we shall present a new computational procedure for obtaining values of surface tension and contact angle from the shape of axisymmetric fluid interfaces. This method differs from previous ones in the following respects:

The objective function, in the optimization scheme, is a measure of the discrepancy between the calculated Laplacian curve and the measured curve. This function is the sum of the squares of the "normal" distances between the measured points and the calculated curve.

The location of the apex of the drop is

assumed unknown and the coordinates of the origin are regarded as independent variables of the objective function. The drop shape, thus, can be measured from any convenient reference frame (see Fig. 2) and any measured point on the surface (either branch of the meridian section) is equally important.

To use the technique, no particular values are required for any parameters, i.e., the surface tension, the radius of curvature at the apex, and the coordinates of the origin (see details below), as they are generated within the program itself, if the user so wishes.

The minimization of the objective function requires solving numerically a system of nonlinear algebraic equations. The numerical scheme employed is a combination of the incremental loading technique and the Newton–Raphson method (11). The function and the derivatives, first and second, are calculated by numerical integration. The integrands are all determined analytically, and therefore the derivatives do not suffer a loss of accuracy.

Finally, this numerical procedure unifies both the method of the sessile drop and the method of the pendant drop. There is no need for any table nor is there any restriction on the applicability of the method.

II. THEORY

When the radii of curvature are sufficiently large, compared to the thickness of a nonhomogeneous film separating two bulk phases, the pressure difference across a curved interface is described by the classical Laplace equation

$$\gamma\left(\frac{1}{R_1}+\frac{1}{R_2}\right)=\Delta P, \qquad [1]$$

where γ is the interfacial tension, R_1 and R_2 represent the two principle radii of curvature, and ΔP is the pressure difference across the interface.

In the absence of external forces, other than gravity, the pressure difference is a linear function of the elevation

$$\Delta P=\Delta P_0+(\Delta\rho)gz, \qquad [2]$$

where ΔP_0 is the pressure difference at a selected datum plane, $\Delta\rho$ is the difference in the densities of the two bulk phases, g is the gravitational acceleration, and z is the vertical height measured from the datum plane.

Referring to Fig. 1, the x axis is tangent to the curved interface and normal to the axis of symmetry and the origin is placed at the apex, then from [1] and [2],

$$\gamma\left(\frac{1}{R_1}+\frac{\sin\phi}{x}\right)=\frac{2\gamma}{R_0}+(\Delta\rho)gz, \qquad [3]$$

where R_1 turns in the plane of the paper and $R_2=x/\sin\phi$ rotates in a plane perpendicular to the plane of the paper and about the axis of symmetry; R_0 is the radius of curvature at the origin of the x–z coordinate system ($R_1=R_2=R_0$ at the origin), and ϕ is the turning angle measured between the tangent to the interface at the point (x, z) and the datum plane.

Mathematically, the interface is described completely as $u=u(x, y, z)$. Due to the symmetry in the system, this may be reduced to the description (shown in Fig. 1) of the meridian section alone. A suitable representation of the meridian curve is in a parametric form

$$x=x(s) \quad \text{and} \quad z=z(s), \qquad [4]$$

s being the arc length measured from the origin, o. In this representation both x and z are single-valued functions of s.

A geometrical consideration yields the differential identities

$$\frac{dx}{ds}=\cos\phi, \qquad [5]$$

and

$$\frac{dz}{ds}=\sin\phi. \qquad [6]$$

By definition

$$\frac{1}{R_1}=\frac{d\phi}{ds} \qquad [7]$$

is the rate of change of the turning angle ϕ with respect to the arc-length parameter s.

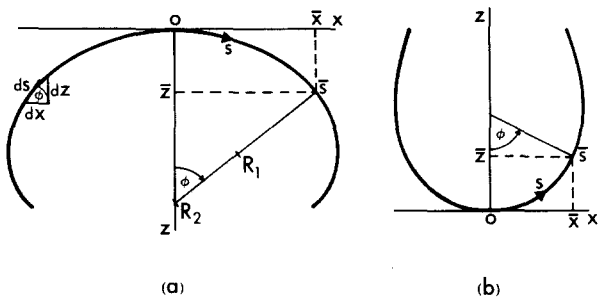

FIG. 1. Definition of the coordinate system. (a) Profile of a sessile drop; (b) Profile of a pendant drop.

Hence, combining [7] with [3] and rearranging yields

$$\frac{d\phi}{ds} = \frac{2}{R_0} + \frac{(\Delta\rho)\cdot g}{\gamma} z - \frac{\sin\phi}{x}. \qquad [8]$$

Equations [5], [6], and [8], and the boundary conditions

$$x(0) = z(0) = \phi(0) = 0, \qquad [9]$$

form a set of first-order differential equations for x, z, and ϕ as functions of the argument s. For given R_0 and given $(\Delta\rho)g/\gamma$ the complete shape of the curve may be obtained by integrating simultaneously these three equations.

III. THE OBJECTIVE FUNCTION

Suppose that u_n, $n = 1, 2, \ldots, N$ are a set of experimental points which describe the meridian section of an interface and $v = v(s)$ is a calculated Laplacian curve. The objective function is defined as

$$E = 1/2 \sum_{n=1}^{N} [d(u_n, v)]^2, \qquad [10]$$

where $d(u_n, v)$ is the normal distance between u_n and the curve v; see Fig. 2. The value of the objective function depends on the shape of the curve v, and on its position relative to the measured curve u. The shape of the curve is determined, as shown above, from the values of R_0 and the slope of the curvature $(\Delta\rho)g/\gamma$. The position of the curve v, relative to the measured curve u, is fixed by the location of the origin (X_0, Z_0). It can be shown that the value of the function will assume a minimum value corresponding to the correct shape of the curve and the correct positioning of the origin. The method of achieving these objectives is described below.

IV. MATHEMATICAL FORMULATION

The transformation of the coordinates, x, z, and s into dimensionless coordinates proves fruitful. Such a transformation will transform the system of Eqs. [5], [6], and [8] into a one-parameter family of curves.

Define

$$\mathscr{s} = \frac{s}{R_0}, \quad \mathscr{x} = \frac{x}{R_0}, \quad \mathscr{z} = \frac{z}{R_0}, \qquad [11]$$

then the system of first-order ordinary differential equations becomes

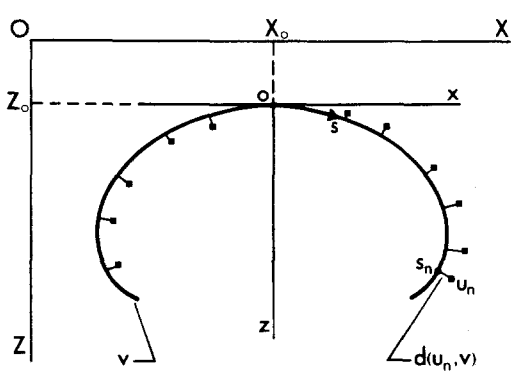

FIG. 2. Schematic of a measured curve and a calculated curve. Experimentally measured points on the interface profile—a calculated Laplacian curve. $d(u_n, v)$ is a normal distance between a point u_n and the curve v.

$$\mathring{x} = \frac{dx}{ds} = \cos\phi,$$

$$\mathring{z} = \frac{dz}{ds} = \sin\phi, \qquad [12]$$

and

$$\mathring{\phi} = \frac{d\phi}{ds} = 2 + \frac{(\Delta\rho)\cdot g\cdot R_0^2}{\gamma} z - \frac{\sin\phi}{x}.$$

In the following analysis, the four parameters which will be regarded as the variables of the objective function E are defined as

$$q_1 = X_0,$$

$$q_2 = Z_0,$$

$$q_3 = R_0, \qquad [13]$$

$$q_4 = \frac{(\Delta\rho)\cdot g\cdot R_0^2}{\gamma},$$

where q_4 ($=\beta$ in (4)), is the shape parameter of the capillary system.

Equation [10] is written as

$$E(q_1, q_2, q_3, q_4) = \sum_{n=1}^{N} e_n(q_1, q_2, q_3, q_4), \quad [14]$$

where

$$e_n = 1/2d(u_n, v)^2.$$

Since all the curves under consideration possess symmetry with respect to the z axis, it is only required to consider one-half of the meridian section. Any datum point which falls on the other portion of the curve can be simply reflected and accounted for by remembering that this point is on the negative (with respect to q_1) side. This is accomplished by using the positive sign in [15] for $X_n \geqq q_1$ and using the negative sign for $X_n < q_1$.

The objective function [14] is the summed squares of all the distances between a calculated curve and the data points. Therefore, it is sufficient to develop the analysis for one single datum point and simplify the notation by eliminating the subscript n.

For the nth datum point, the error is written as

$$e = 1/2\cdot[(q_3\cdot x(s_m, q_4) \pm (q_1 - X))^2 + (q_3\cdot z(s_m, q_4) + q_2 - Z)^2], \quad [15]$$

where

$$q_3\cdot x(s_m, q_4) = x$$

and

$$q_3\cdot z(s_m, q_4) = z,$$

are the coordinates of a point on the curve v which is closest to the experimental point (X, Z) and s_m is the corresponding value of the arc length s at that point.

The value of s_m at which e is evaluated is determined in the following manner: The distance between every point on the calculated curve—for which the values of q_1, q_2, q_3, and q_4 are fixed—and a datum point is regarded as a function of the argument s, say, $f(s)$. This function, f, exhibits a single minimum value at the point where the distance between a datum point and the curve v, is normal to v. The corresponding value of $s = s_m$ at that minimum is used in [15] above. A mathematical statement of the above is

$$\frac{\partial f}{\partial s} \equiv 0, \qquad [16]$$

at constant q_1, q_2, q_3, and q_4.

From the definition in [15], it follows that at constant parameters q_1, q_2, q_3, and q_4:

$$\frac{\partial f}{\partial s} \equiv 0 \equiv \frac{\partial e}{\partial s_m}. \qquad [17]$$

Moreover it is clear that the value of s_m will vary for different values of q_1, q_2, and q_4. Therefore, s_m itself is a function of these variables. Equation [15] can be rewritten as

$$e = e(s_m(q_1, q_2, q_4), q_1, q_2, q_3, q_4). \quad [18]$$

The conditions of an extremum in the value of the error function, Eq. [14], are expressed as

$$\frac{\partial E}{\partial q_k} = \sum_{n=1}^{N} \frac{\partial e_n}{\partial q_k} = 0, \quad k = 1, 2, 3, 4, \quad [19]$$

where for a single nth datum point

$$\frac{\partial e}{\partial q_k} = \left(\frac{\partial e}{\partial \delta_m}\right)\frac{\partial \delta_m}{\partial q_k} + \left(\frac{\partial e}{\partial q_k}\right); \qquad [20]$$

$(\partial e/\partial \delta_m)$ is interpreted as the derivative of e with respect to δ_m at constant values of q_1, q_2, q_3, and q_4. Similarly, $(\partial e/\partial q_k)$ are the derivatives of e with respect to q_k at fixed δ_m.

By invoking relation [17], the first term on the right-hand side in [20] is eliminated. The extremum conditions [19] take the form

$$\frac{\partial E}{\partial q_k} = \sum_{n=1}^{N}\left(\frac{\partial e_n}{\partial q_k}\right) = 0. \qquad [21]$$

V. NEWTON–RAPHSON METHOD

The system of Eq. [21] constitutes a set of nonlinear algebraic equations in the parameters q_1, q_2, q_3, and q_4. Generally, in order to solve for these parameters, an iterative procedure of solution must be employed. A powerful and well-known iterative technique is the Newton–Raphson method (11)

$$\mathbf{Q}^{i+1} = \mathbf{Q}^i - \Delta^i, \quad i = 0, 1, \ldots, I, \qquad [22]$$

where $\mathbf{Q}^i = (q_1, q_2, q_3, q_4)^i$ is the vector the components of which are the unknown parameters at the ith step of the iteration scheme; $\Delta^i = (\delta q_1, \delta q_2, \delta q_3, \delta q_4)^i$ is a correction vector which results from solving the system of linear equations

$$\mathbf{E}(\mathbf{Q}^i)\cdot\Delta^i = \mathbf{E}(\mathbf{Q}^i); \qquad [23]$$

$\mathbf{E}(\mathbf{Q}^i)$ is a vector whose components are the nonlinear expressions $\partial E/\partial q_k$ obtained from Eq. [21], and evaluated at the ith step, and $\mathbf{E}(\mathbf{Q}^i)$ is a $k \times k$ symmetric matrix. The components of the Hessian matrix $\mathbf{E}$ are computed as

$$\frac{\partial^2 E}{\partial q_k \partial q_l} = \sum_{n=1}^{N}\frac{\partial^2 e_n}{\partial q_k \partial q_l}, \qquad [24]$$

where for a single nth datum point

$$\frac{\partial^2 e}{\partial q_k \partial q_l} = \left(\frac{\partial^2 e}{\partial \delta_m^2}\right)\frac{\partial \delta_m}{\partial q_k}\frac{\partial \delta_m}{\partial q_l} + \left(\frac{\partial^2 e}{\partial \delta_m \partial q_l}\right)\frac{\partial \delta_m}{\partial q_k} + \left(\frac{\partial e}{\partial \delta_m}\right)\frac{\partial^2 \delta_m}{\partial q_k \partial q_l} + \left(\frac{\partial^2 e}{\partial q_k \partial \delta_m}\right)\frac{\partial \delta_m}{\partial q_l} + \left(\frac{\partial^2 e}{\partial q_k \partial q_l}\right). \qquad [25]$$

In [25], the expressions for the partial derivative of δ_m with respect to q_k are derived from Eq. [17] which provides an implicit functional relation among the variables of δ_m.

Differentiating Eq. [17],

$$d\left(\frac{\partial e}{\partial \delta_m}\right) = \left(\frac{\partial^2 e}{\partial \delta_m^2}\right)d\delta_m + \sum_{j=1}^{N}\left(\frac{\partial^2 e}{\partial \delta_m \partial q_j}\right)dq_j = 0, \qquad [26]$$

therefore,

$$\frac{\partial \delta_m}{\partial q_k} = -\left(\frac{\partial^2 e}{\partial \delta_m \partial q_k}\right)\Big/\left(\frac{\partial^2 e}{\partial \delta_m^2}\right). \qquad [27]$$

Using Eqs. [17] and [27], Eq. [25] is simplified,

$$\frac{\partial^2 e}{\partial q_k \partial q_l} = \left(\frac{\partial^2 e}{\partial q_k \partial q_l}\right) - \left(\frac{\partial^2 e}{\partial \delta_m \partial q_k}\right)\left(\frac{\partial^2 e}{\partial \delta_m \partial q_l}\right)\Big/\left(\frac{\partial^2 e}{\partial \delta_m^2}\right), \qquad [28]$$

where the brackets in each term in the above equations indicate partial differentiation, with respect to the shown variables, as opposed to the total partial differential of e.

The explicit expressions of the partial derivatives which appear in Eqs. [21] and [28] are shown in Appendix A.I.

VI. INCREMENTAL LOADING METHOD

The major disadvantage of the Newton–Raphson method is that a convergence to the optimum value of the function is ensured provided the starting values of the variables are sufficiently close to the optimal values. Otherwise, if poor initial values are used, the method may fail altogether. An appealing scheme which eliminates the above weakness of the Newton–Raphson method is achieved by combining the method with the method of incremental loading (11). The application of the method to the current problem is described below.

We begin by considering one of the variables of the objective function as a loading

parameter. For fixed value of that parameter, the optimum state of E is determined using the Newton–Raphson iterations. Once the optimum value of E is achieved, the loading parameter together with the variables are incremented to a new value by the incremental loading step and the optimization procedure is repeated. By controlling the increments of the loading parameter to sufficiently small values the variables at the end of a loading step will represent a good initial guess that convergence will take place. The method is terminated once the global optimum of the objective function is found. For the applicability of the method, it is required that a solution to an initial unloaded state of the system will be known. This solution will be described first.

Let q_4 be chosen as the loading parameter. With $q_4 = 0$ ($\gamma \rightarrow \infty$), the Laplacian curve describes a circular curve. The optimum of the function E corresponds to a best fit of a circular arc through the measured points. For this simple case, a simplified objective function may be defined

$$E = 1/2 \sum_{n=1}^{N} (d_n - R)^2, \qquad [29]$$

where R is a mean radius of a circle which is fitted to the data points, and it is defined as

$$R = \frac{1}{N} \sum_{n=1}^{N} d_n \qquad [30]$$

and

$$d_n = [(X_n - X_0)^2 + (Z_n - Z_0')^2]^{1/2} \qquad [31]$$

is the distance between the nth datum point and the center of the circle (X_0, Z_0').

At that point, the objective function reduces to a function of two variables. The values of X_0 and Z_0' which yield the global minimum of [29] must be obtained. The optimization scheme of [29] follows a similar path to that of Eq. [14]; it is required that

$$\frac{\partial E}{\partial X_0} = \frac{\partial E}{\partial Z_0'} = 0. \qquad [32]$$

The numerical solution involves a combination of the method of incremental loading and the Newton–Raphson method. In this case, X_0 is chosen as the loading parameter.

Initially, the center of the circle is located on a Z axis passing through the centroid of the domain of the data points. The best location for the initial center is selected among several calculated positions on this axis.

In the following steps, the value of Z_0', for fixed X_0, is determined using a Newton–Raphson iteration for a function of one variable. The combined steps follow a procedure similar to the one described below in conjunction with the optimization of [14].

When the relative change in the value of E (Eq. [29]) or the values of the derivatives in [32] fall below a threshold value of 10^{-9}, the optimization is terminated. The first value of $\mathbf{Q}^0$ has the components

$$\begin{aligned} q_1 &= X_0, \\ q_2 &= Z_0 = Z_0' - R, \\ q_3 &= R, \\ q_4 &= 0. \end{aligned} \qquad [33]$$

This completes the solution to the unloaded state of the system and a second phase, the incremental loading of q_4, begins.

In the combined loading steps and Newton–Raphson steps, the iteration formula of [22] is modified:

$$\begin{aligned} &\mathbf{Q}^{j,i+1} = \mathbf{Q}^{j,i} - \mathbf{\Delta}^{j,i}, \\ &j, i = 0, 1, \cdots (J, I), \end{aligned} \qquad [34]$$

with the initial value $\mathbf{Q}^{0,0} = \mathbf{Q}^0$.

The vector $\mathbf{\Delta}^{j,i}$ is the solution of the linear system of Eq. [23], written here as

$$\mathbf{E}^{j,i} \cdot \mathbf{\Delta}^{j,i} = \mathbf{E}^{j,i}. \qquad [35]$$

The components of $\mathbf{E}^{j,i}$ and $\mathbf{E}^{j,i}$ are as described previously but with $k = 1, 2, 3$; j is a counter of the loading steps and i is the counter of the Newton–Raphson steps.

At the beginning of every loading step, a

new value of the increment load is determined; q_4 is modified accordingly;

$$q_4^{j+1} = q_4^j - \alpha \cdot \delta q_4^j, \qquad [36]$$

where δq_4^j is obtained by solving the system of Eq. [23] with $\mathbf{Q}^{j,I}$ and $k = 4$ and where α is a damping factor, $0 < \alpha \leqq 1$. For $\alpha = 1$, the increment of q_4 amounts to a full Newton–Raphson step in that variable.

Next, the values of q_1, q_2, and q_3 are readjusted, to obtain the next initial vector $\mathbf{Q}^{j+1,0}$, using Eqs. [34] and [35] but with a modified right-hand side vector in [35],

$$\frac{\partial E^{j+1,I}}{\partial q_k} = \frac{\partial E^{j,I}}{\partial q_k} - \frac{\partial^2 E^{j,I}}{\partial q_k \partial q_4} \alpha \cdot \delta q_4^j, \qquad [37]$$

where all the derivatives are evaluated at $\mathbf{Q}^{j,I}$. As in the case of the unloaded solution, a termination of the optimization is reached if either the relative change of the function value E in Eq. [14] or the derivatives in Eq. [19] are less than the threshold value of 10^{-9}.

At the end of the optimization procedure $\mathbf{Q}^{J,I}$ contains the required information on the correct shape of the Laplacian curve and the correct positioning of the curve relative to the experimental curve. Any additional information about the capillary system can be easily obtained by integration of [12], and utilizing the correct values of the parameters in $\mathbf{Q}^{J,I}$.

VII. THE SYSTEM OF DIFFERENTIAL EQUATIONS

So far, the functions $x(s, q_4)$ and $z(s, q_4)$, as well as the derivatives of these functions, were used as if they were known explicitly. However, all that is known or can be obtained analytically are the differential form of these functions and the differential form of their derivatives. The function values must be obtained by a numerical integration. In this section, the system of differential equation is developed and the method of integration is described.

The differential system of equations in [12] is written here again,

$$\begin{aligned} \dot{x} &= \cos\phi, \\ \dot{z} &= \sin\phi, \\ \dot{\phi} &= 2 + q_4 z - \sin\phi / x, \end{aligned} \qquad [38]$$

or in a compact form as

$$\dot{\mathbf{X}} = \mathbf{F}(\mathbf{X}), \qquad [39]$$

where $\mathbf{X} = (x, z, \phi)$ and the dot denotes a total derivative of $\mathbf{X}$ with respect to s.

The values for $x = q_3 x$ and $z = q_3 z$, which are the coordinates of a point on v, at a point closest to the nth datum point, are defined once Eq. [39] is integrated from $s = 0$ to the value of $s = s_m$.

The terms x' and z', where the prime symbol is used for the operator d/dq_4, were introduced in the expressions for the derivatives of e with respect to q_4 (see Appendix A.I). These terms are not readily available but can be obtained upon integrating the system of equations

$$\begin{aligned} \dot{x}' &= -\phi' \sin\phi, \\ \dot{z}' &= \phi' \cos\phi, \\ \dot{\phi}' &= \frac{\sin\phi}{x^2} x' + z + q_4 z' - \frac{\cos\phi}{x} \phi', \end{aligned} \qquad [40]$$

which is the differential of [38] with respect to q_4. Collectively, Eqs. [40] are written as

$$\dot{\mathbf{X}}' = \mathbf{G}(\mathbf{X}, \mathbf{X}'), \qquad [41]$$

where

$$\mathbf{X}' = (x', z', \phi').$$

The values of x' and z' are known at the point m once Eq. [41] is integrated from $s = 0$ to $s = s_m$.

Similarly, in the expressions for the second derivatives of e with respect to q_4, the terms x'' and z'' are needed. These terms, again, are not readily available but can be obtained by integrating the system

$$\begin{aligned} \dot{x}'' &= -(\phi')^2 \cos\phi - \phi'' \sin\phi, \\ \dot{z}'' &= -(\phi')^2 \sin\phi + \phi'' \cos\phi, \\ \dot{\phi}'' &= -2 \frac{\sin\phi}{x^3} (x')^2 + 2 \frac{\cos\phi}{x^2} x'\phi' \\ &\quad + \frac{\sin\phi}{x^2} x'' + 2z' + q_4 z'' \\ &\quad + \frac{\sin\phi}{x} (\phi')^2 - \frac{\cos\phi}{x} \phi''. \end{aligned} \qquad [42]$$

These relations are determined by differentiating Eqs. [40].

In vector form Eqs. [42] are written as

$$\mathring{\mathbf{X}}'' = \mathbf{H}(\mathbf{X}, \mathbf{X}', \mathbf{X}''), \qquad [43]$$

where $\mathbf{X}$ and $\mathbf{X}'$ were already defined and $\mathbf{X}'' = (\varkappa'', \varkappa'', \phi'')$. Once again, the terms $\varkappa''$ and $\varkappa''$ are known quantities at $\sigma = \sigma_m$ when [43] is integrated from $\sigma = 0$ to the value of $\sigma = \sigma_m$.

Equations [39], [41], and [43] together form a single system of first-order ordinary differential equations,

$$\mathring{\mathbf{V}}(\sigma) = \mathbf{U}(\sigma, \mathbf{V}(\sigma)), \qquad [44]$$

where $\mathbf{V} = (v_1, v_2, \ldots, v_9) = (\mathbf{X}, \mathbf{X}', \mathbf{X}'')$ and $\mathbf{U}$ is the vector of the differential equations $\mathbf{U} = (\mathbf{F}, \mathbf{G}, \mathbf{H})$.

Any one of several numerical integration techniques can be used for the integration of [44]. In this work the method of numerical integration used falls under the classification of a second-order implicit Euler method of integration (Appendix B). In that method of integration, the approximation $\mathbf{V}^k$ to $\mathbf{V}(\mathbf{X}^k, \mathbf{X}'^k, \mathbf{X}''^k)$ is obtained from the recursion formula

$$\mathbf{V}^{k+1} = \mathbf{V}^k + \Delta^k, \quad k = 0, 1, \ldots, k, \qquad [45]$$

where Δ^k is an incremental vector $\Delta^k = (\Delta\mathbf{X}^k, \Delta\mathbf{X}'^k, \Delta\mathbf{X}''^k)$, and is the solution of the linear system of equations

$$\left(\mathbf{I} - \frac{\Delta\sigma}{2}\mathbf{U}_v\right)\Delta^k = \Delta\sigma\left(\mathbf{U} + \frac{\Delta\sigma}{2}\mathbf{U}_\sigma\right). \qquad [46]$$

Here $\mathbf{I}$ is the identity matrix, $\Delta\sigma$ is an incremental step in the arc-length coordinate σ, and $\mathbf{U}_v$ is a matrix of derivatives of $\mathbf{U}$ with respect to the variables v_i and is written as

$$\mathbf{U}_v = \begin{bmatrix} \mathbf{A} & 0 & 0 \\ \mathbf{B} & \mathbf{A} & 0 \\ \mathbf{C} & 2\mathbf{B} & \mathbf{A} \end{bmatrix}. \qquad [47]$$

In [46], $\mathbf{U}_\sigma = 0$ since σ is not present in the expressions of $\mathbf{U}$ explicitly and in [47] the matrices $\mathbf{A}$, $\mathbf{B}$, and $\mathbf{C}$ are submatrices of the Jacobian of $\mathbf{U}$ and are shown explicitly in Appendix A.II.

The solution of [46] can be simplified by taking advantage of the special structure of $\mathbf{U}$. The following sequence of three equations is replacing the system [46]: First, determine $\Delta\mathbf{X}^k$ from

$$\underset{\sim}{\mathbf{A}}\Delta\mathbf{X}^k = (\Delta\sigma)\mathbf{F}; \qquad [48]$$

next, determine $\Delta\mathbf{X}'^k$ from

$$\underset{\sim}{\mathbf{A}}\Delta\mathbf{X}'^k = (\Delta\sigma)\mathbf{G} + \frac{\Delta\sigma}{2}\mathbf{B}(\Delta\mathbf{X}^k);$$

and finally, solve for $\Delta\mathbf{X}''^k$ from

$$\underset{\sim}{\mathbf{A}}\Delta\mathbf{X}''^k = (\Delta\sigma)\mathbf{H} + \frac{\Delta\sigma}{2}[\mathbf{C}(\Delta\mathbf{X}^k) + 2\mathbf{B}(\Delta\mathbf{X}'^k)],$$

where $\underset{\sim}{\mathbf{A}} = \left(\mathbf{I} - \frac{\Delta\sigma}{2}\mathbf{A}\right)$.

The first increment step Δ^0 is determined by expanding $\mathbf{V}$ into a Taylor series about the point $\sigma = 0$ and neglecting terms of order $(\Delta\sigma)^3$ to obtain

$$\Delta\mathbf{X}^0 = (\Delta\sigma, 1/2(\Delta\sigma)^2, \Delta\sigma),$$
$$\Delta\mathbf{X}''^0 = \Delta\mathbf{X}''^0 = 0. \qquad [49]$$

VIII. ON THE IMPLEMENTATION OF THE COMPUTATIONAL PROCEDURE

The computational procedure which is described above has been programmed for computer use in FORTRAN and tested on an IBM 370: The flow chart is shown in Fig. 3. The program consists of a set of subroutines and is self-sufficient.

Subroutine INTFCE is called by the user. This subroutine handles the optimization procedure, of the combined methods of incremental loading and the Newton–Raphson method, where q_4 is the loading parameter.

Subroutine INIT is called by INTFCE. In INIT, the first vector $\mathbf{Q}^0$ and an integration step length $\Delta\sigma$ are determined, from the data which the user provided.

Subroutine INTFCE calls next subroutine SYSEQ. In SYSEQ, the error function Eq. [14] is constructed, the components of the vector $\mathbf{E}$ and the components of the Hessian

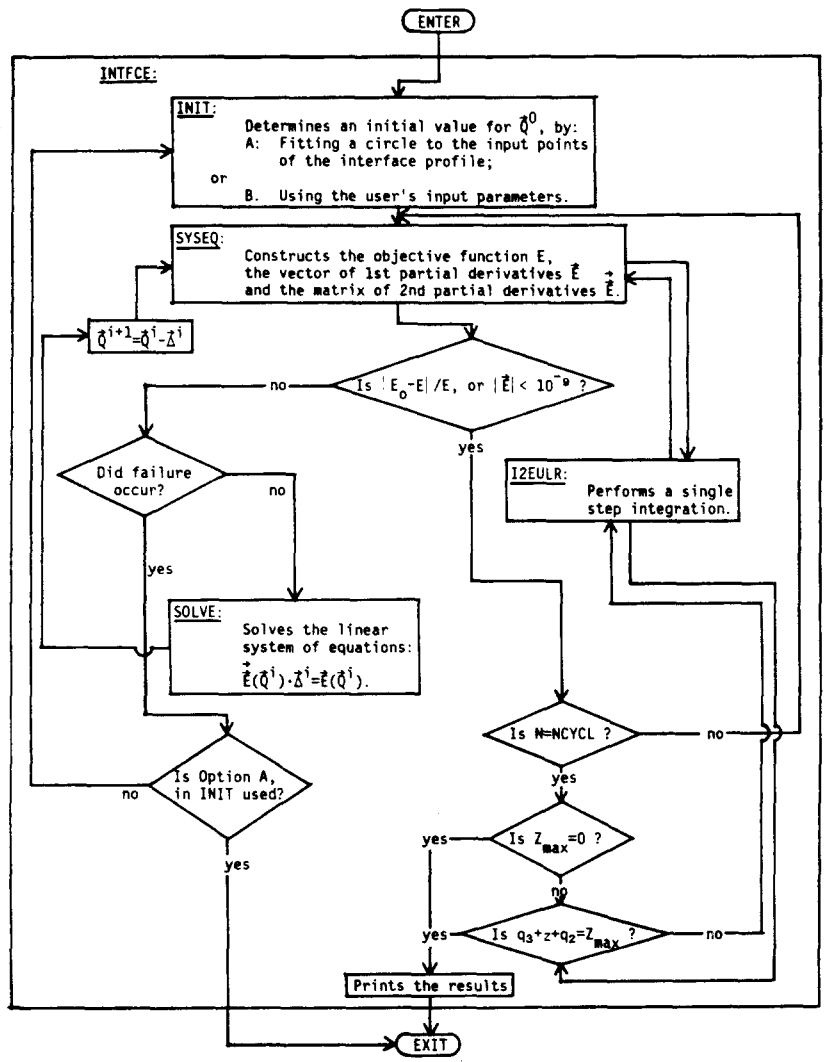

FIG. 3. Flow chart.

matrix **E** of Eq. [23]. In the course of constructing these terms, subroutine SYSEQ calls subroutine I2EULR where the integration scheme of [48] is performed.

On return from SYSEQ, subroutine INTFCE calls subroutine SOLVE where the solution of [23] or [35] is performed. Once the optimizing vector $\mathbf{Q}^{J,I}$ is finally determined, the optimization procedure is terminated. The accuracy of the numerically computed values of $\mathbf{Q}^{J,I}$ can be checked internally by repeating the above optimization procedure and using, in the new round of computation, the previous value of $\mathbf{Q}^{J,I}$ as a first vector $\mathbf{Q}^0$ in INTFCE. In the new round of the computation the integration step length, DELS, is reduced to half its previous value.

The value of the contact angle, if desired, is calculated in INTFCE which performs the integration of [38] by calling subroutine I2EULR. The computed values of the surface tension, the value of the contact angle, and the values of the coordinates of the apex point are printed by INTFCE.

The experimental points (X_n, Z_n), $n = 1$,

. . . , N needed as input data can be measured from an arbitrary X–Z coordinate system, as shown in Fig. 2, where the X axis is perpendicular to the axis of symmetry of the interface; Z is measured positive in the direction away from the X axis and into the concave side of the interface.

The values of the density difference, $\Delta\rho$ ($\Delta\rho > 0$), between the bulk phases, the magnitude of the local gravitational acceleration, g, and the values of X_0, Z_0, R_0, and γ are required. The gravitational acceleration vector is assigned positive for sessile drops, and it is assigned negative for pendant drops.

The value of the surface tension may be specified as zero. The parameters X_0, Z_0, and R_0 (equivalent to q_1, q_2, and q_3) will then be determined within the program, regardless of their specified values as was previously outlined for the solution of the unloaded state of the system with $q_4 = 0$. For routine work, this strategy is recommended. However, for certain purposes, such as statistical analysis of results good values of γ_{LV} may already be available, and it will then be more efficient (computer time!) to assign a nonzero value to the surface tension and the other parameters. In this case, a good value of $\mathbf{Q}^0$ is already known, and the optimization scheme with a nonzero q_4 as the loading parameter will proceed. But if several consecutive iteration steps will fail to converge, possibly due to bad initial value of $\mathbf{Q}^0$, this phase of the optimization will be abandoned. The algorithm will start from the beginning, as if a zero value of γ had been specified.

The listing of the program may be purchased from the authors.

IX. NUMERICAL EXAMPLES

A. Sessile Drop

Using the tables of Bashforth and Adams (4), we have selected the situation

$$\beta = g \cdot R_0^2(\Delta\rho)/\gamma = 25,$$
$$\phi = 110°,$$
$$\bar{x}/R_0 = 0.47345,$$
$$\bar{z}/R_0 = 0.31665,$$

where $\bar{x}$ (see Fig. 1a) is the radius of curvature in a horizontal plane passing through a point $\bar{s}$ on the surface of the drop and $\bar{z}$ is the vertical distance from the apex of the drop to the horizontal plane.

Suppose that a drop has a base that coincides with the horizontal plane through $\bar{s}$; then ϕ is the corresponding contact angle, $\bar{x}$ is the contact diameter of that drop, and $\bar{z}$ is the maximum drop height above the surface.

Next, a specific value of surface tension and of density difference are considered:

$$\gamma = 72.785 \text{ ergs/cm}^2$$

(e.g., water at 20°C),

$$\Delta\rho = 0.9982 \text{ g/cm}^3.$$

From the information given above, an interface configuration is constructed via a numerical integration of the system of Eqs. [5], [6], and [8]. The parameters R_0 and $(\Delta\rho)g/\gamma$ are determined for each case and using a fourth-order Runge–Kutta integration routine, the entire surface is described. Next, a set of data points is arbitrarily selected from the resulting curve to represent "experimental" points.

B. Pendant Drop

A similar procedure to that described in A is used for generating a profile of a pendant drop (Fig. 1b). Using the tables of Fordham (5) for pendant drops, the value of β and corresponding values of $\bar{x}/R_0$ and $\bar{z}/R_0$ are selected and the system of Eqs. [5], [6], and [8] is integrated. From the resulting curve a set of data points is considered as well as one additional point which will be used to determine the maximum height, Z_{max}, between the apex of the drop and the supporting surface.

The corresponding parameters are

$$\beta = -0.275,$$
$$\bar{x}/R_0 = 1.02867,$$
$$\bar{z}/R_0 = 1.41077,$$

and

$$\phi = 123.004°, \quad \text{at} \quad Z_{max} = 0.30668 \text{ cm}.$$

The values of surface tension and density difference are those specified above.

At this stage the prepatory steps are completed and the method of solution which is described earlier can be examined:

The input information to the program consists of the following:

—set of data points: (X_n, Z_n), $n = 1, \ldots, N$;

—density difference, gravitational acceleration vector, assumed value of surface tension, X_0, Z_0, R_0, and value of Z_{max};

—control parameters such as the number of partitions of one-half the meridian section, the number of repetitions of the optimization procedure, and the total number of data points.

In both cases, the values of $X_0 = Z_0 = R_0 = \gamma = 0$ are used.

When each run is completed, the values of the parameters q_1, q_2, q_3, q_4 that correspond to a best fit of a calculated curve to the measured curve are obtained. The value of the surface tension is then determined,

$$\gamma = (\Delta\rho)g(q_3)^2/q_4, \qquad [50]$$

and the contact angle is the angle ϕ obtained by proceeding with the integration of [38] until $z = Z_{max} - q_2$ is satisfied.

The results are given in Figs. 4 and 5.

X. DISCUSSION

A novel computation scheme for determining interfacial tensions from the shapes of axisymmetric liquid–fluid interfaces is developed.

The method of solution is versatile and is not restricted by any particular drop shape or drop size. It is shown that whether the drop is a sessile drop (Fig. 4) or a pendant drop (Fig. 5), the cases are treated in a unified manner.

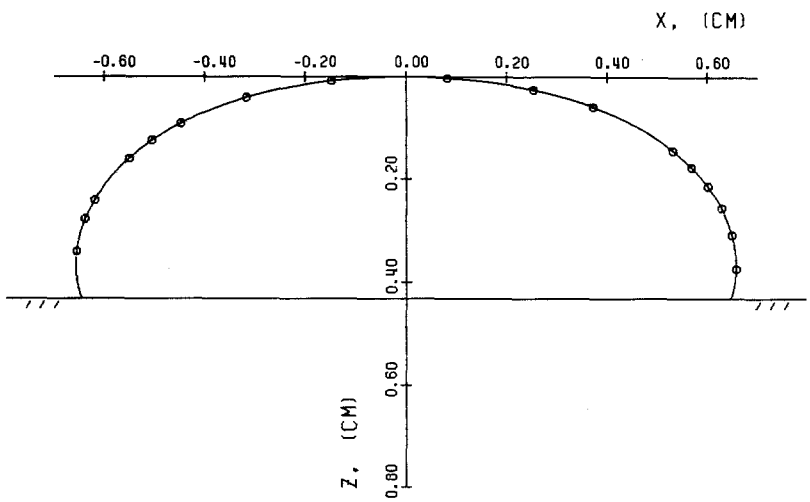

FIG. 4. A profile of a sessile drop.

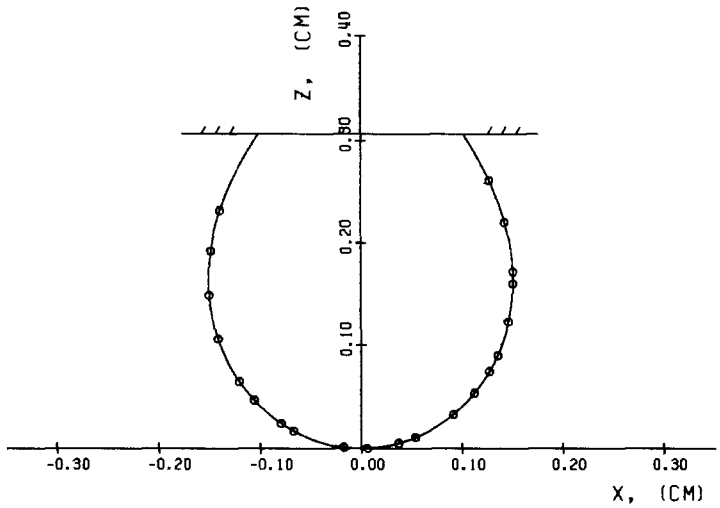

FIG. 5. A profile of a pendant drop.

The amount of physical input data that is required is kept to a minimum. It consists of the values of the coordinate points of the discretized interface, the value of the density difference across the interface and the value of the local acceleration of gravity.

The method can be extended easily to generate other quantities of physical interest such as the surface area of the interface and the volume of the drop.

APPENDIX A: MATHEMATICAL RELATIONS

I. Partial Derivatives of the Objective Function

The function e for a single datum point is expressed as

$$e = 1/2[q_3 x(s, q_4) \pm (q_1 - X))^2 + (q_3 z(s, q_4) + q_2 - Z)^2]. \quad [A.1]$$

The following is a list of partial derivatives which are used in the definitions of Eqs. [21] and [28]. The notation $\mathring{x}$ is used for the differential $\partial x/\partial s$ and the notation x' is used for the differential $\partial x/\partial q_4$:

$$\frac{\partial e}{\partial s} = (q_3 x \pm (q_1 - X))q_3 \mathring{x} + (q_3 z + q_2 - Z)q_3 \mathring{z}, \quad [A.2]$$

$$\frac{\partial^2 e}{\partial s^2} = (q_3 x \pm (q_1 - X))q_3 \mathring{\mathring{x}} + (q_3 z + q_2 - Z)q_3 \mathring{\mathring{z}} + q_3^2, \quad [A.3]$$

$$\frac{\partial^2 e}{\partial s \partial q_1} = \pm q_3 \mathring{x} \quad \text{(positive sign for } X \geqq q_1 \text{ and negative sign for } X < q_1), \quad [A.4]$$

$$\frac{\partial^2 e}{\partial s \partial q_2} = q_3 \mathring{z}, \quad [A.5]$$

$$\frac{\partial^2 e}{\partial s \partial q_3} = (q_3 x \pm (q_1 - X))\mathring{x} + (q_3 z + q_2 - Z)\mathring{z} + q_3(x\mathring{x} + z\mathring{z}), \quad [A.6]$$

$$\frac{\partial^2 e}{\partial \mathscr{s}\,\partial q_4} = (q_3\varkappa \pm (q_1 - X))q_3(\mathring{\varkappa})' + (q_3\varkappa + q_2 - Z)q_3(\mathring{\varkappa})' + q_3^2(\varkappa'\mathring{\varkappa} + \varkappa'\mathring{\varkappa}), \quad [A.7]$$

$$\frac{\partial e}{\partial q_1} = \pm(q_3\varkappa \pm (q_1 - X)), \quad [A.8]$$

$$\frac{\partial e}{\partial q_2} = q_3\varkappa + q_2 - Z, \quad [A.9]$$

$$\frac{\partial e}{\partial q_3} = (q_3\varkappa \pm (q_1 - X))\varkappa + (q_3\varkappa + q_2 - Z)\varkappa, \quad [A.10]$$

$$\frac{\partial e}{\partial q_4} = (q_3\varkappa \pm (q_1 - X))q_3\varkappa' + (q_3\varkappa + q_2 - Z)q_3\varkappa', \quad [A.11]$$

$$\frac{\partial^2 e}{\partial q_1^2} = 1, \quad [A.12]$$

$$\frac{\partial^2 e}{\partial q_1 \partial q_2} = 0, \quad [A.13]$$

$$\frac{\partial^2 e}{\partial q_1 \partial q_3} = \pm\varkappa, \quad [A.14]$$

$$\frac{\partial^2 e}{\partial q_1 \partial q_4} = \pm q_3', \quad [A.15]$$

$$\frac{\partial^2 e}{\partial q_2^2} = 1, \quad [A.16]$$

$$\frac{\partial^2 e}{\partial q_2 \partial q_3} = \varkappa, \quad [A.17]$$

$$\frac{\partial^2 e}{\partial q_2 \partial q_4} = q_3\varkappa', \quad [A.18]$$

$$\frac{\partial^2 e}{\partial q_3^2} = \varkappa^2 + \varkappa^2, \quad [A.19]$$

$$\frac{\partial^2 e}{\partial q_3 \partial q_4} = (q_3\varkappa \pm (q_1 - X))\varkappa' + (q_3\varkappa + q_2 - Z)\varkappa' + q_3(\varkappa\varkappa' + \varkappa\varkappa'), \quad [A.20]$$

$$\frac{\partial^2 e}{\partial q_4^2} = (q_3\varkappa \pm (q_1 - X))q_3\varkappa'' + (q_3\varkappa + q_2 - Z)q_3\varkappa'' + q_3^2(\varkappa'^2 + \varkappa'^2). \quad [A.21]$$

II. Matrices Appearing in the Integration Scheme

The explicit form of the three submatrices **A**, **B**, and **C** of Eq. [47] are

$$\mathbf{A} = \begin{bmatrix} 0 & 0 & -\sin\phi \\ 0 & 0 & \cos\phi \\ \dfrac{\sin\phi}{\varkappa^2} & q_4 & -\dfrac{\cos\phi}{\varkappa} \end{bmatrix}, \quad [A.22]$$

$$\mathbf{B} = \begin{bmatrix} 0 & 0 & -\phi' \cdot \cos\phi \\ 0 & 0 & -\phi' \cdot \sin\phi \\ \left(-2\dfrac{\sin\phi}{\varkappa^3}\varkappa' + \dfrac{\cos\phi}{\varkappa^2}\phi'\right) & 1 & \left(\dfrac{\cos\phi}{\varkappa^2}\varkappa' + \dfrac{\sin\phi}{\varkappa}\phi'\right) \end{bmatrix}, \quad [A.23]$$

$$\mathbf{C} = \begin{bmatrix} 0 & 0 & (\phi^2 \sin\phi - \phi'' \cos\phi) \\ 0 & 0 & (-\phi'^2 \cos - \phi'' \sin\phi) \\ \left(6\dfrac{\sin\phi}{\varkappa^4}\varkappa'^2 - 4\dfrac{\cos\phi}{\varkappa^3}\varkappa'\phi - 2\dfrac{\sin\phi}{\varkappa^3}\varkappa'' - \dfrac{\sin\phi}{\varkappa^2}\phi'^2 + \dfrac{\cos\phi}{\varkappa^2}\phi''\right) & 0 & \left(-2\dfrac{\cos\phi}{\varkappa^3}\varkappa'^2 - 2\dfrac{\sin\phi}{\varkappa^2}\varkappa'\phi' + \dfrac{\cos\phi}{\varkappa^2}\varkappa'' + \dfrac{\cos\phi}{\varkappa}\phi'^2 + \dfrac{\sin\phi}{\varkappa}\phi''\right) \end{bmatrix}. \quad [A.24]$$

APPENDIX B: NUMERICAL INTEGRATION: A SECOND-ORDER IMPLICIT EULER METHOD

Considering a system of first-order ordinary differential equations

$$\mathring{\mathbf{X}} = \mathbf{F}(t, \mathbf{X}), \qquad [B.1]$$

where

$$\mathbf{X} = \begin{Bmatrix} x_1 \\ x_2 \\ \vdots \\ x_n \end{Bmatrix}$$

and

$$\mathbf{F}(t, \mathbf{X}(t)) = \begin{Bmatrix} f_1(t, \mathbf{X}) \\ f_2(t, \mathbf{X}) \\ \vdots \\ f_m(t, \mathbf{X}) \end{Bmatrix};$$

$\mathbf{F}$ is assumed sufficiently differentiable with respect to both t and $\mathbf{X}$, and $\mathbf{X}(t_0) = \mathbf{X}_0$.

Expanding $\mathbf{X}(t)$ into a Taylor series about the point $t_0 + \Delta t$ yields

$$\mathbf{X}(t_0 + \Delta t) = \mathbf{X}(t_0) + \Delta t\mathring{\mathbf{X}}(t_0) + 1/2(\Delta t)^2\mathring{\mathring{\mathbf{X}}}(t_0) + O(\Delta t)^3. \qquad [B.2]$$

The second derivative of $\mathbf{X}$ with respect to t can be expressed by taking the total derivative of $\mathbf{F}$ with respect to t; thus

$$\mathring{\mathring{\mathbf{X}}} = \mathbf{F}_t + \mathbf{F}_x\mathring{\mathbf{X}}, \qquad [B.3]$$

where

$$\mathbf{F}_t = \frac{\partial}{\partial t}[\mathbf{F}(t, \mathbf{X})] \qquad [B.4]$$

and

$$\mathbf{F}_x = \begin{bmatrix} f_{1x_1} \cdots f_{1x_2} \cdots f_{1x_n} \\ \vdots \quad \vdots \quad \vdots \\ f_{mx_1} \cdots f_{mx_2} \cdots f_{mx_n} \end{bmatrix}. \qquad [B.5]$$

Next, express

$$\mathring{\mathbf{X}}(t_0) = \frac{\mathbf{X}(t_0 + \Delta t) - \mathbf{X}(t_0)}{\Delta t} + O(\Delta t) = \frac{\Delta \mathbf{X}}{\Delta t} + O(\Delta t) \qquad [B.6]$$

and substitute [B.6] into [B.3]

$$\mathring{\mathring{\mathbf{X}}} = \mathbf{F}_t + \mathbf{F}_x\frac{\Delta \mathbf{X}}{\Delta t} + O(\Delta t). \qquad [B.7]$$

Substituting [B.7] into the series [B.2] and rearranging:

$$\Delta \mathbf{X} = (\Delta t)\mathbf{F} + 1/2(\Delta t)^2 \times \left(\mathbf{F}_t + \mathbf{F}_x\frac{\Delta \mathbf{X}}{\Delta t}\right) + O(\Delta t)^3. \qquad [B.8]$$

Solving for $\Delta \mathbf{X}$ and neglecting terms of $O(\Delta t)^3$, find

$$\mathbf{X}(t_0 + \Delta t) = \mathbf{X}(t_0) + \Delta \mathbf{X}, \qquad [B.9]$$

where $\Delta \mathbf{X}$ is the solution of the system of equations

$$(\mathbf{I} - 1/2(\Delta t)\mathbf{F}_x)\Delta \mathbf{X} = (\Delta t)\mathbf{F} + 1/2(\Delta t)^2\mathbf{F}_t. \qquad [B.10]$$

REFERENCES

1. Padday, J. F., *in* "Surface and Colloid Science" (E. Matijević and F. R. Eirich, Eds.), Vol. 1. Wiley–Interscience, New York, 1969.
2. Ambwani, D. S., and Fort, Jr., T., *in* "Surface and Colloid Science" (R. J. Good and R. R. Stromberg, Eds.), Vol. 11, pp. 93–119. Plenum, New York, 1979.
3. Neumann, A. W., and Good, R. J., *in* "Surface and Colloid Science" (R. J. Good and R. S. Stromberg, Eds.), Vol. 11, pp. 31–91, Plenum, New York, 1979.
4. Bashforth, F., and Adams, J. C., "An Attempt to Test the Theory of Capillary Action." Cambridge Univ. Press and Deighton Bell & Co., Cambridge, 1892.
5. Fordham, S., *Proc. Roy. Soc. London A* **194,** 1 (1948).
6. Stauffer, C. E., *J. Phys. Chem.* **69,** 1933 (1965).
7. Hartland, S., and Hartley, R. W., "Axisymmetric Fluid–Liquid Interfaces." Elsevier, Amsterdam, 1976.
8. Malcolm, J. D., and Paynter, H. M., *J. Colloid Interface Sci.* **82,** 269–275 (1981).
9. Maze, C., and Burnet, G., *Surface Sci.* **13,** 451 (1969).
10. Maze, C., and Burnet, G., *Surface Sci.* **24,** 335 (1971).
11. Ortega, J. M., and Rheinboldt, W. C., "Iterative Solution of Nonlinear Equations in Several Variables." Academic Press, New York, 1970.